University of Glasgow

Shire, T. and Standing, J. (2021) Strength and stiffness properties of an unsaturated clayey silt: experimental study at high degrees of saturation. *International Journal of Geomechanics*, 21(7), 04021094.
(doi: 10.1061/(ASCE)GM.1943-5622.0002049)

The material cannot be used for any other purpose without further permission of the publisher and is for private use only.

There may be differences between this version and the published version. You are advised to consult the publisher's version if you wish to cite from it.

http://eprints.gla.ac.uk/229103/

Deposited on 22 January 2021

Enlighten – Research publications by members of the University of Glasgow
http://eprints.gla.ac.uk

Strength and stiffness properties of an unsaturated clayey silt: experimental study at high degrees of saturation

Tom Shire [1*] and Jamie Standing[2]

[1]James Watt School of Engineering, University of Glasgow, UK
[2]Department of Civil and Environmental Engineering, Imperial College London, UK

* thomas.shire@glasgow.ac.uk

Abstract

Unsaturated constant water content triaxial compression tests with suction measurement using an Imperial College Tensiometer, and saturated consolidated undrained tests were carried out on reconstituted Brickearth, a naturally unsaturated clayey silt from London. The results show that the saturated effective stress can be applied to the critical state line (CSL) and normalised stiffness for unsaturated Brickearth but that Bishop's effective stress variable gives a slightly improved CSL. The stiffness derived from local instrumentation demonstrates that Bishop's effective stress is also beneficial for normalising the stiffness modulus over the small strain range (up to axial strains of about 3%).

Introduction

Unsaturated soils are commonly found in arid/tropical regions and to a lesser extent in temperate regions, and in compacted fill materials. Mechanical testing of soils in an unsaturated state presents experimental challenges, in particular relating to the measurement of suction and volume change. Various experimental techniques can be adopted to overcome these such as the use of double-walled cells for volume measurement (Wheeler 1988) and the axis-translation technique for suction control with positive pore water pressures and elevated air pressures (Fredlund et al. 2012; Thu et al. 2006; Toll and Ong 2003). Constant water content triaxial testing, in which air drainage is permitted but water drainage is not is a convenient technique for testing under conditions similar to many field situations, in which the air phase can be considered drained and the water phase undrained (Thu et al. 2006). The use of a high capacity tensiometer for suction measurement (Mendes and Toll 2016; Ridley and Burland 1993) allows accurate matrix suction measurement and reduces the overall test duration in comparison with the axis-translation technique (Marinho et al. 2016). Other techniques, such as relative humidity control, are still necessary to reach very high suction values e.g. Patil et al. (2016).

This paper presents the results from unsaturated constant water content and saturated consolidated undrained triaxial compression tests, performed at Imperial College London, on reconstituted Brickearth, an unsaturated loessic clayey silt. The intention of testing reconstituted specimens was to allow the effects of degree of saturation, expressed in terms of soil suction, on sample behaviour to be isolated and assessed without the influence of soil structure. The shear strength and stiffness behaviour of the Brickearth are analysed considering the effect of mean stress and pore water pressure. Tests on the unsaturated specimens were performed with two Imperial College tensiometers in contact with the soil, thus allowing the direct measurement of suction and the uniformity of suctions within the specimen during shearing to be checked, neither of which are possible when using the axis-translation technique. Local strain measurement allows sample stiffness to be measured in the small strain range (ε < 0.1%), which is common in saturated soil testing but much less so in unsaturated soils (e.g. Ng and Xu 2012). Local strain measurement in unsaturated soils also allows sample volume and therefore degree of saturation to be monitored accurately, allowing the change in Bishop's effective stress to be determined during shearing. The results are assessed in relation to the saturated critical state line and Bishop's effective stress variable (Bishop et al. 1960).

Materials and methods

Brickearth

Brickearth, or Langley Silt Member (Milodowski et al. 2015), is an unsaturated yellow-brown clayey silt which is found as a superficial loessic deposit across southern Britain. Block samples of the soil tested here were retrieved from beneath St Paul's Cathedral, London, during excavation of a shaft to provide lift access to the crypt. The soil consists of 19% clay, 70% silt and 11% sand. The liquid limit, w_{LL} = 31% and plasticity index, I_P = 13%, give a classification of low plasticity clay. Further details can be found in Wong et al. (2019).

Specimen reconstitution

Disturbed samples of the Brickearth were dried and ground to a powder using a mechanical pestle and mortar. The powder was thoroughly mixed into a slurry with demineralised water at 1.25w_{LL} (Burland 1990). Following a period of one week to allow for complete hydration, the slurry was consolidated in a 229-mm diameter consolidometer under an applied vertical stress of 200 kPa. The resulting cake was removed from the consolidometer and specimens trimmed using a wire saw initially and then shaped using a soil lathe and end trimmer, techniques used to minimise sample disturbance.

Filter paper testing

The filter paper technique (Chandler and Gutierrez 1986) was used to determine soil water retention curves (SWRC) in terms of matrix suction vs. degree of saturation, void ratio and gravimetric water content. Discs of 100 mm diameter and 20 mm thickness were trimmed from the cake prepared in the consolidometer. Dry Whatman 42 filter papers were placed directly in contact at the flat faces of the soil discs and which were then sealed with cling film and wax. The discs were allowed to equilibrate at zero total stress under stable temperature and humidity conditions for two weeks before being unwrapped to measure filter paper water content (Al Haj and Standing 2016). The relationship between filter paper water content and suction proposed by Chandler and Gutierrez (1986) was used. Three discs, taken from the top, middle and bottom of the consolidometer cake, were dried and then wetted in stages to determine a full SWRC. No differences were noted between the SWRCs determined from each position in the cake.

Saturated triaxial testing

Conventional consolidated undrained (CU) compression triaxial testing was carried out on three samples of 50 mm diameter and 100mm height, trimmed from the consolidated cake. High resolution local instrumentation was used to measure accurately axial and radial deformations at small strains (two axial LVDTs, linear variable differential transformers (Cuccovillo and Coop 1997), and a radial belt). Samples were initially saturated by increasing the cell pressure under undrained conditions to achieve a Skempton pore pressure coefficient, B = 0.97 and then isotropically consolidated to the required value of mean effective stress, p', before being sheared at an axial strain rate of 5 %/day. Properties of the CU samples prior to shearing are presented in Table 1. The samples had values of initial mean effective stress, p'_0 = 200, 350 and 500 kPa respectively.

Unsaturated triaxial testing

Constant water content (CWC) triaxial compression tests (Marinho et al. 2016; Mendes and Toll 2016) were carried out on three 50-mm diameter samples trimmed from the consolidated cake using the same process as the CU samples. Again high resolution local instrumentation was used to measure accurately axial and radial deformation at small strains and these in turn were used to calculate volumetric strain and hence degree of saturation, S_r. The limit to the range over which the local measurements could give accurate measurements was set at an axial strain of ε_a = 3%. A single walled steel cell was used, meaning that nominally volumetric strains could be determined from changes in overall cell volume using a volume gauge connected to it which also controlled the cell pressure. However, in practice, because of the very small magnitude of volumetric strains, this was not sufficiently accurate. Local instrumentation was therefore relied on for accurately determining volumetric strain and hence void ratio and degree of saturation up to ε_a = 3% and final values were obtained by measuring the volume of the samples retrieved at the end of the tests.

Two Imperial College Tensiometers (ICTs) were used to measure locally the (negative) pore water pressure, u_w (Ridley and Burland 1993). Air pressure, u_a, was maintained at atmospheric levels, meaning that matrix suction $s = (u_a - u_w) = -u_w$. The ICTs were placed in direct contact with the sample via grommets inserted through the membrane at two locations midway between the centre and ends of the sample (Figure 1) to measure changes in suction and also check that the shearing rate (5 %/day) was sufficiently low to maintain similar pressure in both ICTs, to ensure that pore pressure gradients along the height of the sample were negligible. The maximum suction that can be measured with such instruments is about 1500 kPa (Ridley and Burland, 1993) but cavitation can occur at lower values depending on factors such as the length of time the suction has been held and the contact of the probe with the sample which sometimes deteriorates because of sample distortion after extended shearing.

The CWC samples were air dried in a controlled temperature laboratory to the required values of initial water content (shown in Table 2), assessed by measurements of overall mass, before being sealed with clingfilm and wax and allowed to equilibrate for a period of at least one week. Values of the initial and final degree of saturation for each test sample are given in Table 2. Sample notation indicates the gravimetric water content and initial mean total stress, p_0. After application of the initial isotropic confining pressure p_0, an equalisation stage followed in which p_0 was maintained until samples came into suction equilibrium and changes in axial and volumetric strain were insignificant, before shearing in axial compression at an axial strain rate of 5 %/day with constant radial total stress σ_r = p_0.

Results

Soil water retention curve

The SWRCs, determined using the filter paper method with additional data from Singhakowin (2015) are presented in terms of degree of saturation in Figure 2a and gravimetric water content in Figure 2b. The apparent air-entry value (Mendes and Toll 2016) is around 75 kPa corresponding to a water content of w = 20% and the limit of the suction which can be measured using the filter paper technique (30 MPa) was reached at a degree of saturation of around S_r = 10%, which corresponds to w = 4%, which is close to the residual (or hygroscopic) value under laboratory conditions. Initial values from the ICTs in the triaxial tests (after the sample was placed in the apparatus but before the application of confining pressure) have also been added to Figure 2, and show excellent agreement with drying data. This might be expected as the triaxial samples were dried from same compacted cake used for the filter paper tests, but is also important as it confirms that the two methods of measuring suction were consistent with each other. Curves have been fitted to the data using the van Genuchten relationship (van Genuchten 1980):

$$w = w_r + \frac{w_s - w_r}{\left(1 + \left(\frac{s}{\alpha}\right)^n\right)^m}$$

Where w_s and w_r are the saturated and residual water contents, s is suction and m, n and α are model parameters where α = 2000, $m = 1.4$ and n = 0.75. The same formulation can be expressed in terms of degree of saturation.

Stress-strain and strength properties

Deviator stress vs. axial strain (q – ε_a) relationships for the CU and CWC samples are presented in Figure 3. The saturated CU samples show increasing ultimate deviator stress with initial mean effective stress and all of them failed in a barrelling mode (as shown in Figure 4a). These saturated CU samples all show lower ultimate deviator stress values than the unsaturated CWC samples, at similar confining stresses, in line with the expected additional strength provided by suction under unsaturated conditions (Fredlund et al. 2012). Based on considerations of constant deviator stress and pore water pressure it can be concluded that each CU sample reached a critical state condition.

There are two very clear trends from the results from the CWC tests. *(i)* two of the samples were sheared under a confining pressure of 200 kPa. The sample with the lower water content (w = 14.5%)

and hence lower degree of saturation, exhibits greater strength and stiffness than the other with w = 16%. *(ii)* two of the samples with the same water content (w = 14.5%) were sheared under different confining stresses (σ_3 = 100 and 200 kPa). The sample under the higher confining stress had a markedly stronger and stiffer response.

In contrast to the other samples, the stress-strain response of sample CWC-14.5-100 (see Figure 3) suggests a strain-softening behaviour with a drop in deviatoric stress at around ε_a = 13%. This is probably related to the formation of a shear band as shown in Figure 4b. CWC-16-200 also shows very minor evidence of strain softening beyond ε_a = 20%. In both these cases where there is either a shear plane present or the sample has distorted significantly at very large strains, the accurate determination of sample area becomes difficult, potentially leading to inaccurate deviator stress values. The other unsaturated sample, CWC-14.5-200, does not show strain softening behaviour, but shearing was terminated at ε_a = 16% due to cavitation of one of the ICTs. If strain-softening were to occur, the samples at the higher confining pressure (200 kPa) would be expected to show less softening. It is not possible to conclude definitively that the CWC samples have reached a critical state, although it appears that they are approaching a state with almost constant deviator stress.

Variations in pore water pressure with axial strain for the unsaturated and saturated samples are shown in Figure 5 (saturated samples started from the same value of 250 kPa, the back pressure applied during the consolidation stage). All samples show an initial sharp increase in pore water pressure upon shearing before levelling off at about $\varepsilon_a \approx 5\%$, after which there is a gradual reduction in values with increasing axial strains. During the initial increase in pore water pressure, suctions (negative pore water pressure) in samples CWC-14.5-200 and CWC-16-200 both reduce to below 50 kPa, with CWC-14.5-100 levelling off at a suction of about 100 kPa, before starting to increase gradually again.

The variation in void ratio for the unsaturated samples up to ε_a = 3%, calculated using the local measurements, is shown in Figure 6. The final values calculated from the post-test sample dimensions are also shown at a nominal strain of ε_a = 20%. After an initial compression, which broadly correlates with the increase in pore water pressure (Figure 5), all samples begin to dilate (again correlating with the gradual decrease in pore water pressure, or increase in suction). It can be inferred from the final void ratio values that the volume change levels off at some point during shearing. Similar observations were made by Jotisankasa et al. (2009).

As the saturated samples were sheared undrained, they did not undergo volumetric strain and so are not shown in Figure 6. However, although there were no volume changes, the sharp increase in pore water pressure in the early stages of shearing shown in Figure 5 would usually be associated with a contractant response, similar to that observed with the unsaturated samples. Equally the subsequent very gradual reduction in pore water pressure with continued shearing would be associated with a dilatant response. Again it is reassuring to see a good correlation in sample response based on the two independent systems for measuring pore water pressure and sample volume change.

The stress paths in $q – p´$ space for the CU samples are shown in Figure 7. The shapes of the stress paths are similar for each sample with an initial reduction in $p´$, correlating with the observed pore water pressure increase, followed by a phase transformation at around ε_a = 5%, (see contours of equal axial strain marked on Figure 7), after which both q and $p´$ increase until critical state conditions are approached.

For the unsaturated CWC samples the stress paths are presented in the q vs. $(p – u_w)$ space in Figure 8. Although $(p – u_w)$ is equivalent to mean effective stress, following Mendes and Toll (2016), the term $p´$ is not used as the samples are not saturated. Here the samples do not exhibit a clear phase transformation but show a slight increase in $(p – u_w)$ as the vertical stress increases during compression slightly outweigh the increases in pore water pressure, which were much smaller than those of the saturated samples. As shearing was performed under constant water content, during the initial stages the degree of saturation of the samples would have increased as they contracted, but from the point that dilation commenced, at an axial strain of about 1%, S_r would have started to decrease as is evident from the final values of S_{rf} determined at the end of the tests (given in Table 2).

The stress paths in $q – (p – u_w)$ space from the CU and CWC tests are compared in Figure 9. The saturated critical state line (CSL) relating to the CU tests has a gradient of M = 1.27. Assuming that the unsaturated CWC samples have reached a critical state, it can be seen that CWC-16-200 and CWC-14.5-200 are in good agreement with the saturated CSL. The stress path for sample CWC-14.5-100 reaches the saturated critical state line (CSL) at peak stress before retreating along a similar path to around q = 400 kPa (the end point of each stress path is marked with a cross). Although this response might be due to inaccuracies in estimating the sample area, as discussed earlier, the closer overall fit to the saturated CSL for the CWC samples can also be explained by considering the degree of saturation and suction values. Table 2 shows the final degree of saturation, S_{rf} for the CWC tests, determined from the final sample mass and dimensions. CWC-16-200 and CWC-14.5-200 have S_{rf} = 81.6 and 75.4% respectively and therefore have greater zones of continuous water. This means that the assumption that the saturated principle of effective stress applies, is closer to reality for these samples than for CWC-14.5-100, which has S_{rf} = 72.3%. To account for degree of saturation in an effective stress framework the modified mean Bishop's stress can be used (Wheeler et al. 2003):

$$p^* = p - S_r\, u_w - (1 - S_r)u_a$$

where u_a is air pressure (as noted earlier, for the CWC tests presented here $u_a = 0$).

The final points for all tests in $q - p^*$ space are shown in Figure 10. Only the final points are plotted, as volume change was not measured reliably throughout the tests and therefore only the final values of S_{rf} could be calculated (from the sample retrieved at the end of each test). It can be seen that all the final points of the unsaturated CWC tests now fall slightly closer to the saturated CSL than when using $p - u_w$, corroborating findings of other researchers (Khalili et al. 2004; Mendes and Toll 2016). This suggests that while the saturated effective stress is a reasonable approximation for saturated soils, Bishop's stress provides a more accurate representation of unsaturated soil behaviour, even at relatively low degrees of saturation (i.e. for $S_r > 72\%$).

It should be noted that with further drying, the water phase would become discontinuous, with only meniscus water existing at particle contacts. The results presented here have only been applied to samples with continuous water phases.

Stiffness properties

The secant modulus, *E*, calculated using the high resolution local instrumentation is plotted against axial strain for all samples in Figure 11(a). There is a greater variation in stiffness for the saturated samples (CU) than the unsaturated samples (CWC): the reason for this is not clear. The secant modulus normalised by $(p - u_w)$ is presented in Figure 11(b). Most stiffness values normalise to a reasonably narrow band with the exception of CU500 at strains smaller than $\varepsilon_a < 0.02\%$, again showing that methods normally applied to fully saturated soils give a reasonable approximation for the mechanics of moderately unsaturated soils. Figure 11(c) shows the secant modulus normalised by p^*. This appears to give a slightly improved fit compared to $E/(p - u_w)$, particularly at very small strains. This is highlighted in Figure 12, which shows the normalised stiffness at $\varepsilon_a < 0.1\%$ for the unsaturated samples only. The samples with $w = 14.5\%$ show excellent agreement when normalised by p^*, and convergence between the samples at different gravimetric water contents occurs at a lower axial strain when normalised by p^* compared to $p - u_w$ ($\varepsilon_a \approx 0.017\%$ and $\varepsilon_a \approx 0.023\%$ respectively).

Summary

This paper presents the results of three saturated consolidated undrained and three unsaturated constant water content triaxial compression tests on reconstituted Brickearth. Local measurements of suction were made on the unsaturated samples using Imperial College Tensiometers. The following conclusions can be drawn from these tests.

a. For saturated samples, ultimate conditions in effective stress in $q - (p - u_w)$ space provide~~s~~ a good approximation of the critical state line. The approximation was not so good for unsaturated samples with final degrees of saturation $S_r < 82\%$, where both air and water are likely to be continuous.

b. Using the modified Bishop's mean stress p^* as a state variable in place of $(p - u_w)$ resulted in a closer agreement between saturated and unsaturated critical states.

c. The secant stiffness normalised by $(p - u_w)$ and p^* resulted in a narrow band of values for saturated and unsaturated soils over the range of degree of saturation considered here, with p^* giving a slightly better normalisation.

Data Availability Statement

The data shown in the graphs in the current study are available at http://dx.doi.org/10.5525/gla.researchdata.914

Acknowledgements

The authors are grateful to the Engineering and Physical Sciences Research Council (EPSRC) who funded the first author through a Doctoral Prize Fellowship. They also wish to thank Mssrs. Steve Ackerley, Graham Keefe and Duncan Parker for their technical support and Dr Tingfa Liu for help with the experiments. The Authors would like to thank the anonymous reviewers whose helpful comments on the original submission significantly strengthened this paper.

References

Bishop, A. W., Alpan, I., Blight, G. E., and Donald, I. B. (1960). "Factors Controlling the Strength of Partly Saturated Cohesive Soils." *Research Conference on Shear Strength of Cohesive Soils*, 503–532.

Burland, J. B. (1990). "On the compressibility and shear strength of natural clays." *Geotechnique*.

Chandler, R. J., and Gutierrez, C. I. (1986). "The filter-paper method of suction measurement." *Geotechnique*, 36(2), 265–268.

Cuccovillo, T., and Coop, M. R. (1997). "The measurement of local axial strains in triaxial tests using LVDTs." *Geotechnique*.

Fredlund, D. G. (Delwyn G. ., Rahardjo, H. (Harianto), and Fredlund, M. D. (2012). *Unsaturated soil mechanics in engineering practice*. John Wiley & Sons.

van Genuchten, M. T. (1980). “A Closed-form Equation for Predicting the Hydraulic Conductivity of Unsaturated Soils.” *Soil Science Society of America Journal*.

Al Haj, K. M. A., and Standing, J. R. (2016). “Soil water retention curves representing two tropical clay soils from Sudan.” *Geotechnique*, Thomas Telford Ltd, 66(1), 71–84.

Jotisankasa, A., Coop, M., and Ridley, A. (2009). “The mechanical behaviour of an unsaturated compacted silty clay.” *Géotechnique*.

Khalili, N., Geiser, F., and Blight, G. E. (2004). “Effective stress in unsaturated soils: Review with new evidence.” *International Journal of Geomechanics*, 4(2), 115–126.

Marinho, F. A. M., Genaro, G. C. G., and Orlando, P. D. G. (2016). “Constant Water Content Compression Tests on Unsaturated Compacted Soil with Suction Measurement Using a HCT.” *International Journal of Geomechanics*, 16(6), 1–15.

Mendes, J., and Toll, D. G. (2016). “Influence of Initial Water Content on the Mechanical Behavior of Unsaturated Sandy Clay Soil.” *International Journal of Geomechanics*, 16(6), D4016005.

Milodowski, A. E., Northmore, K. J., Kemp, S. J., Entwisle, D. C., Gunn, D. A., Jackson, P. D., Boardman, D. I., Zoumpakis, A., Rogers, C. D. F., Dixon, N., Jefferson, I., Smalley, I. J., and Clarke, M. (2015). “The mineralogy and fabric of ‘Brickearths’ in Kent, UK and their relationship to engineering behaviour.” *Bulletin of Engineering Geology and the Environment*, Springer Berlin Heidelberg, 74(4), 1187–1211.

Ng, C. W. W., and Xu, J. (2012). “Effects of current suction ratio and recent suction history on small-strain behaviour of an unsaturated soil.” *Canadian Geotechnical Journal*.

Patil, U. D., Hoyos, L. R., and Puppala, A. J. (2016). “Characterization of compacted silty sand using a double-walled triaxial cell with fully automated relative-humidity control.” *Geotechnical Testing Journal*.

Ridley, A. M., and Burland, J. B. (1994). “A new instrument for the measurement of soil moisture suction.” *Geotechnique*, 44(3), 551–556.

Thu, T. M., Rahardjo, H., and Leong, E. C. (2006). “Shear strength and pore-water pressure characteristics during constant water content triaxial tests.” *Journal of Geotechnical and Geoenvironmental Engineering*, 132(3), 411–419.

Toll, D. G., and Ong, B. H. (2003). “Critical-state parameters for an unsaturated residual sandy clay.” *Geotechnique*, 53(1), 93–103.

Wheeler, S. J. (1988). “The undrained shear strength of soils containing large gas bubbles.” *Géotechnique*, Thomas Telford Ltd , 38(3), 399–413.

Wheeler, S. J., Sharma, R. S., and Buisson, M. S. R. (2003). “Coupling of hydraulic hysteresis and stress–strain behaviour in unsaturated soils.” *Géotechnique*, Thomas Telford Ltd , 53(1), 41–54.

Wong, L. X., Shire, T., and Standing, J. (2019). “Effect of depositional water content on the collapsibility of a reconstituted loess.” *Quarterly Journal of Engineering Geology and Hydrogeology*, Geological Society of London, qjegh2018-025.

Tables

Table 1. Saturated sample properties prior to shearing

Sample	Initial mean effective stress, p_0' (kPa)	Void ratio, e_0	Gravimetric water content, w (%)
CU200	200	0.565	21.0
CU350	350	0.501	18.9
CU500	500	0.481	18.0

Table 2. Unsaturated sample properties

Sample	Initial mean total stress, p_0 (=σ_3) (kPa)	Void ratio prior to test, e_{prep}	Void ratio at start of shearing e_0	Final void ratio (after sample removed from apparatus), e_f	Gravimetric water content, w (%)	Degree of saturation ratio prior to test, S_{rprep} (%)	Degree of saturation ratio at start of shearing S_{r0} (%)	Final degree of saturation (after sample removed from apparatus), S_{rf} (%)
CWC-16-200	200	0.506	0.503	0.530	16.0	85.3	85.6	81.6
CWC-14.5-200	200	0.501	0.489	0.532	14.5	80.2	82.2	75.4
CWC-14.5-100	100	0.498	0.493	0.546	14.5	79.8	80.5	72.3

Figures

Fig. 1. Unsaturated sample with ICTs and radial strain belt (axial LVDTs yet to be fitted).

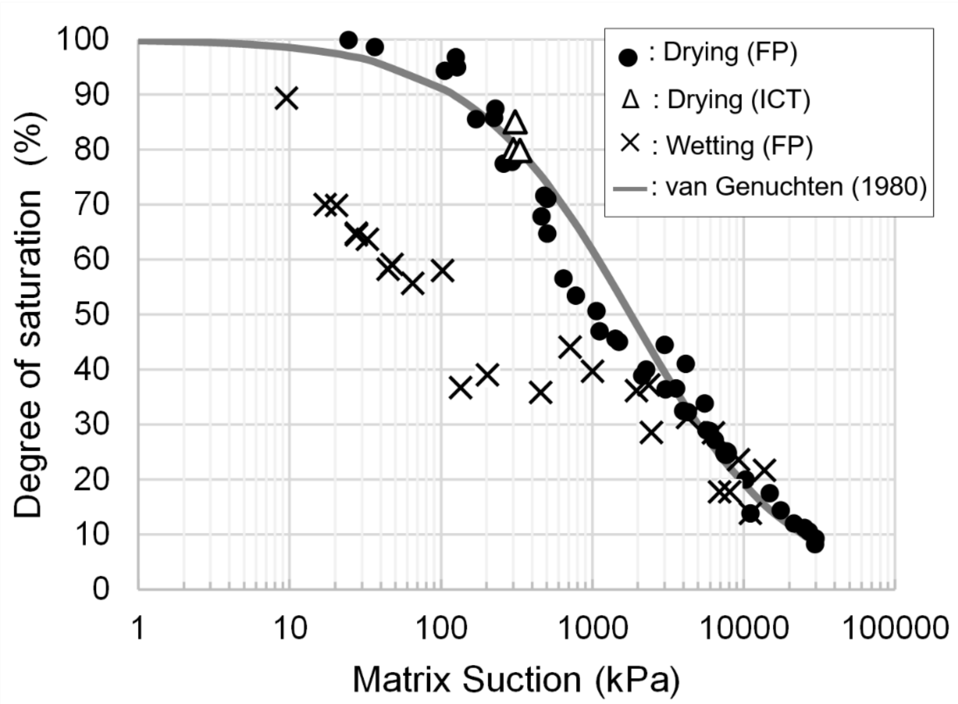

Fig. 2(a)

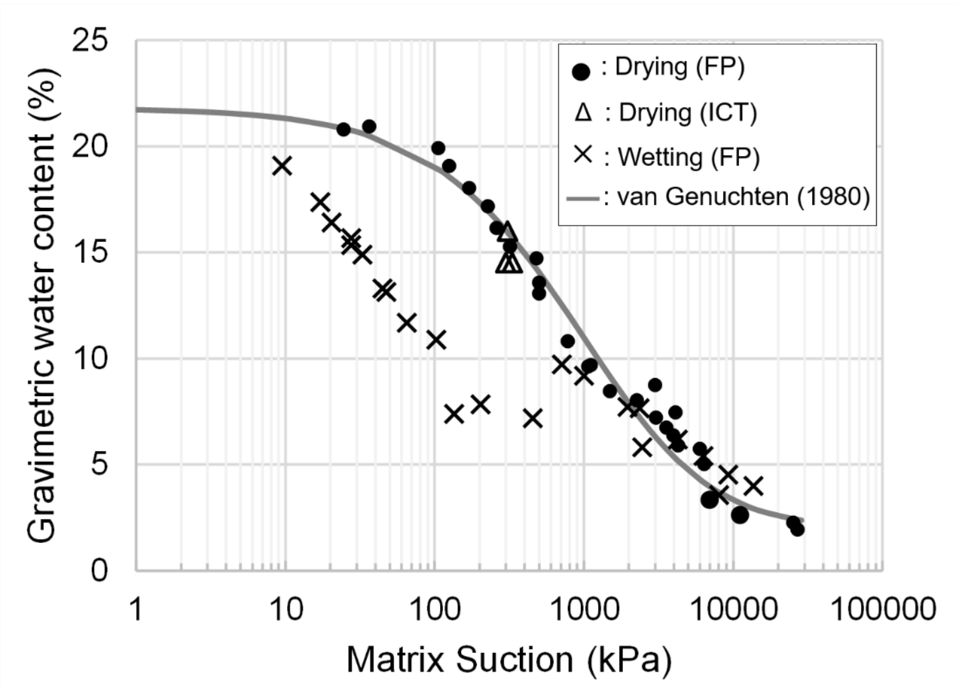

Fig. 2(b)

Fig. 2. Soil water retention curves determined from filter paper test measurements and initial (pre-compression) values from the CWC tests, determined using the ICT: (a) in terms of degree of saturation; (b) in terms of gravimetric water content.

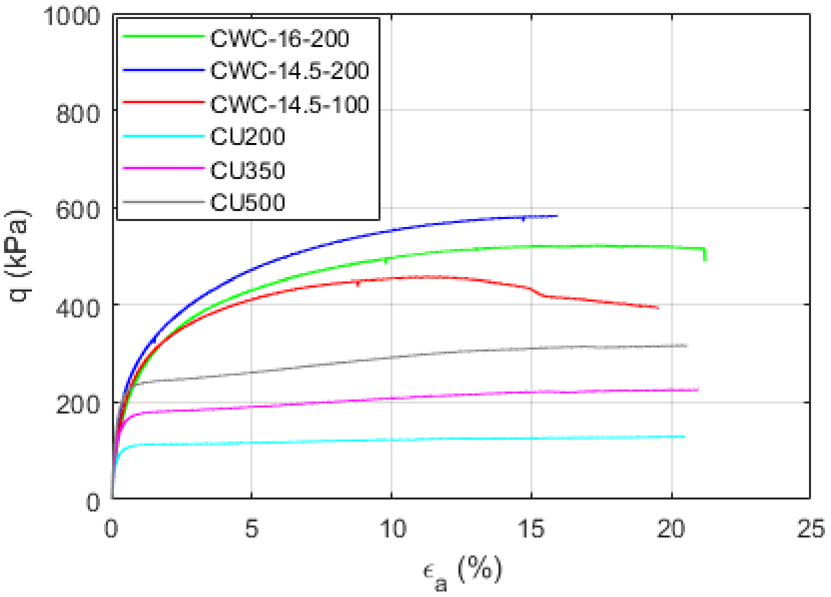

Fig. 3. Deviator stress – axial strain relationships for unsaturated and saturated samples.

Fig. 4. Photographs of samples after shearing: (a) saturated sample CU350; (b) unsaturated sample CWC-14.5-100.

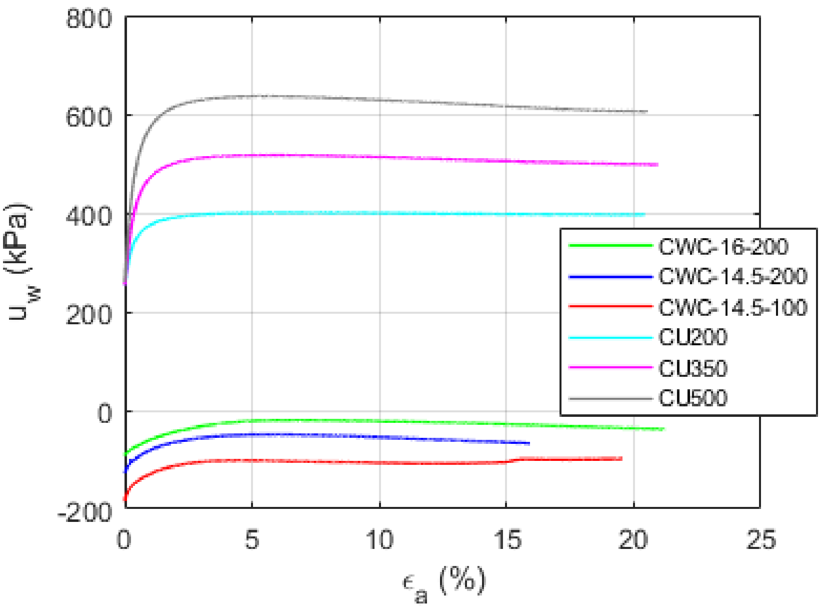

Fig. 5. Pore water pressure – axial strain relationships for unsaturated and saturated samples.

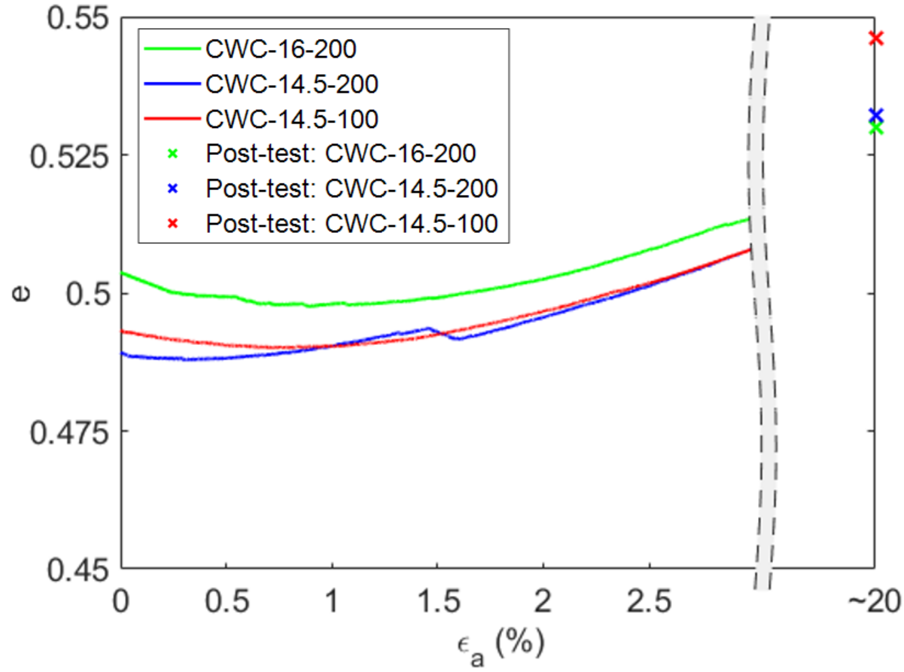

Fig. 6. Void ratio – axial strain relationships for unsaturated and saturated samples. Final void ratio values are plotted at a nominal axial strain of 20%.

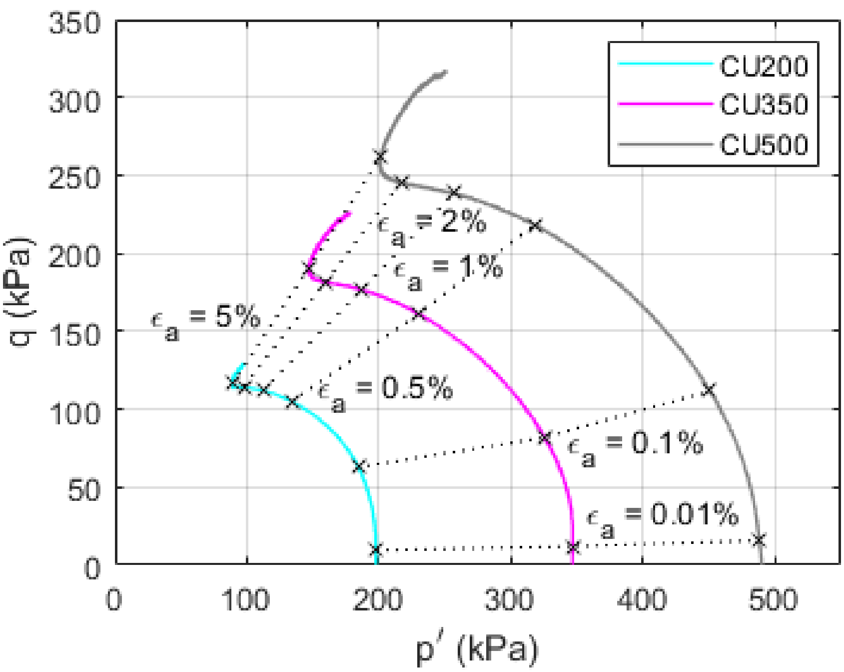

Fig. 7. Stress paths for saturated CU samples in $q - p'$ space with axial strain contours shown.

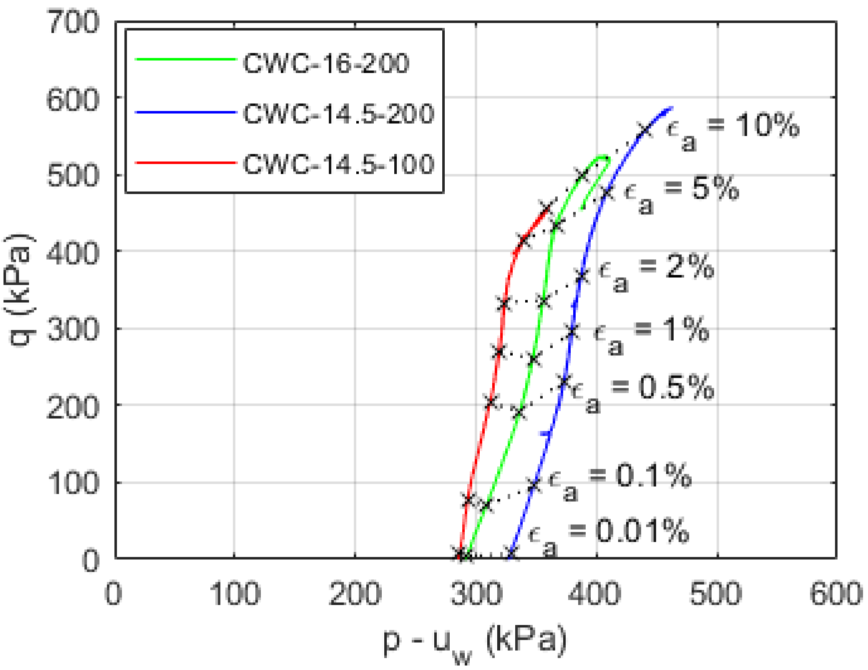

Fig. 8. Stress paths for unsaturated CWC samples in $q - (p - u_w)$ space with axial strain contours shown.

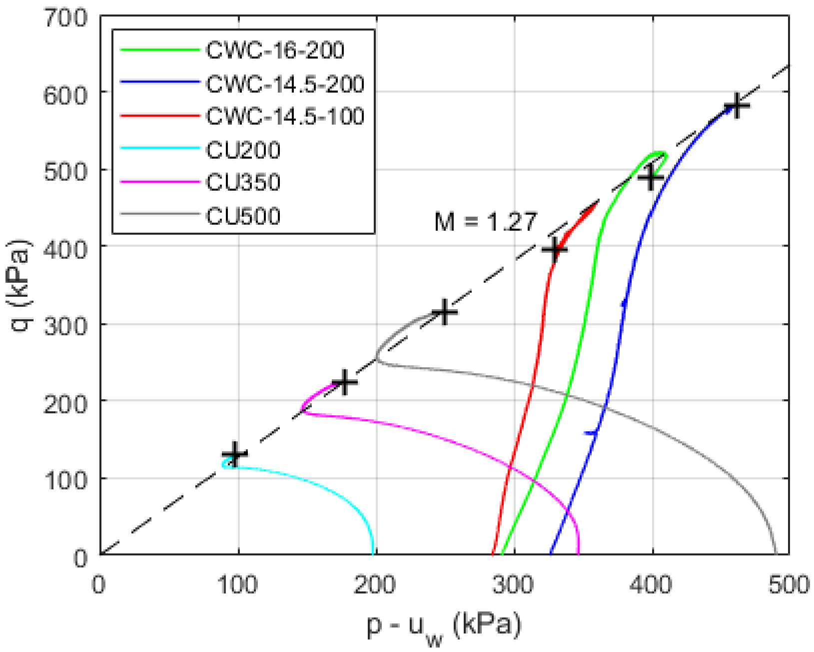

Fig. 9. Stress paths in $q - (p - u_w)$ space for saturated and unsaturated tests. Crosses mark the final stress state in each test.

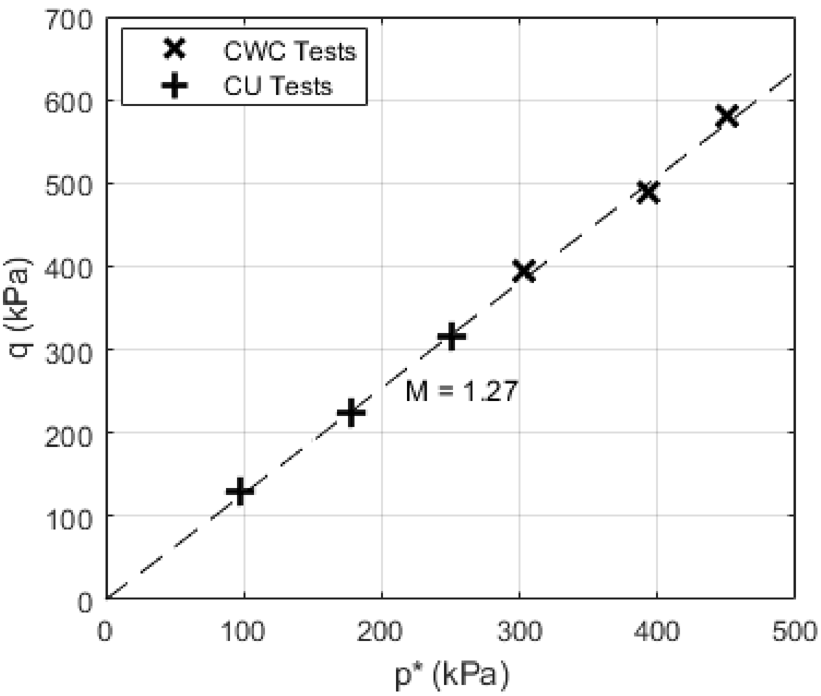

Fig. 10. Final stress points for all tests in $q - p^*$ space.

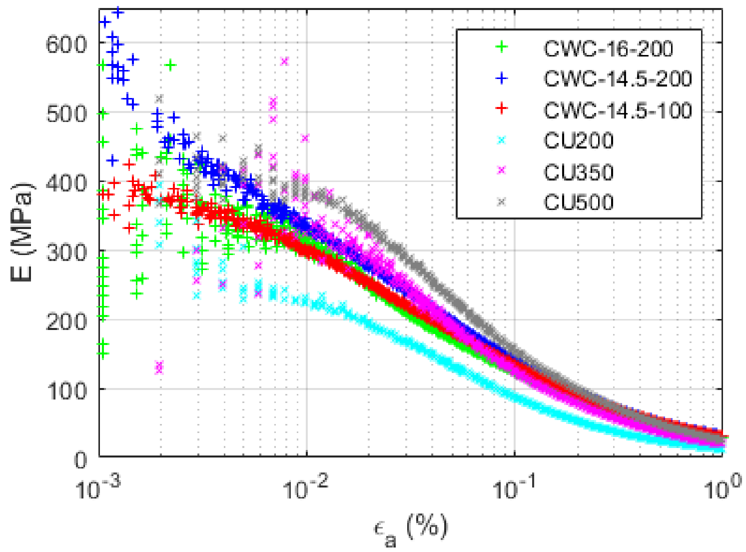

Fig. 11(a)

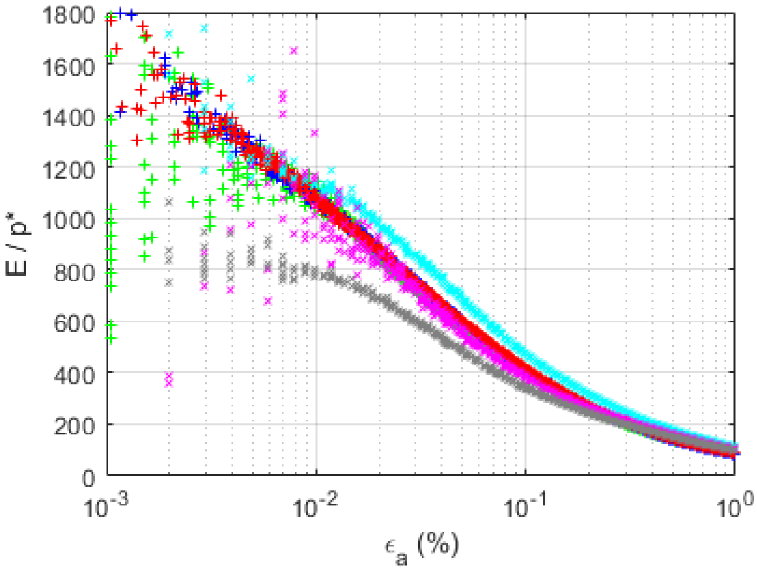

Fig. 11(b)

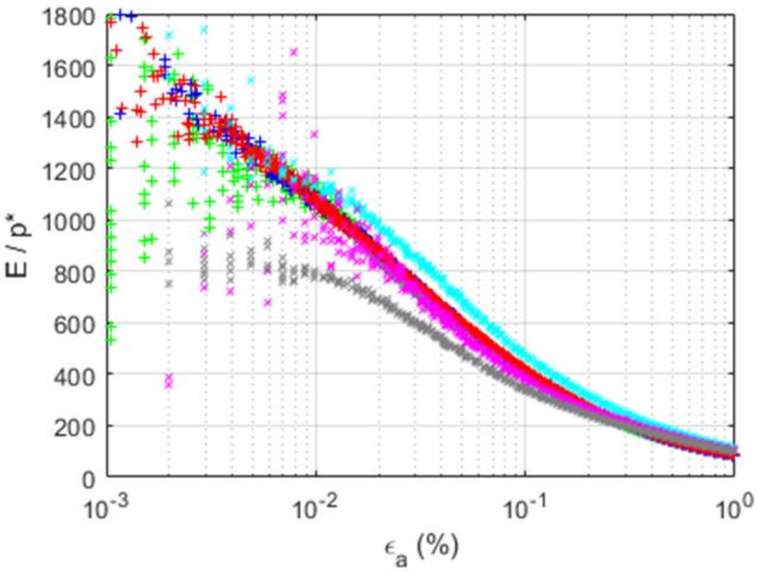

Fig. 11(c)

Fig. 11. Sample stiffnesses: (a) variation of secant modulus with axial strain; (b) values normalised by ($p - u_w$); (c) values normalised by p*.

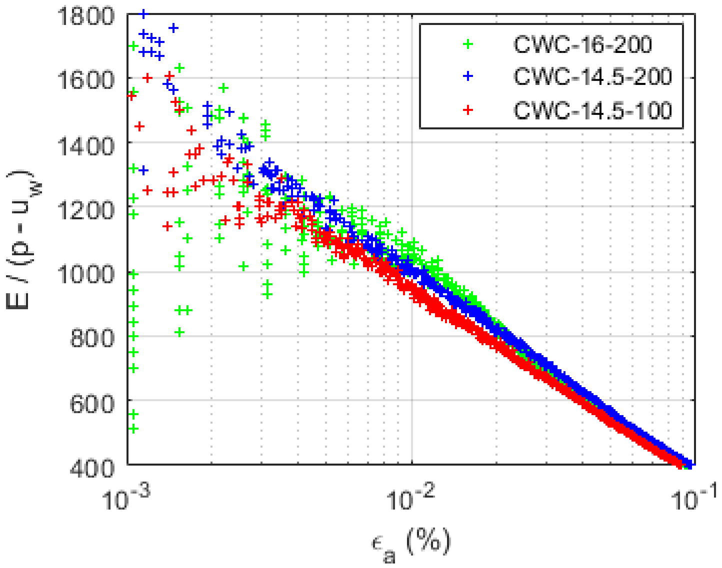

Fig. 12(a)

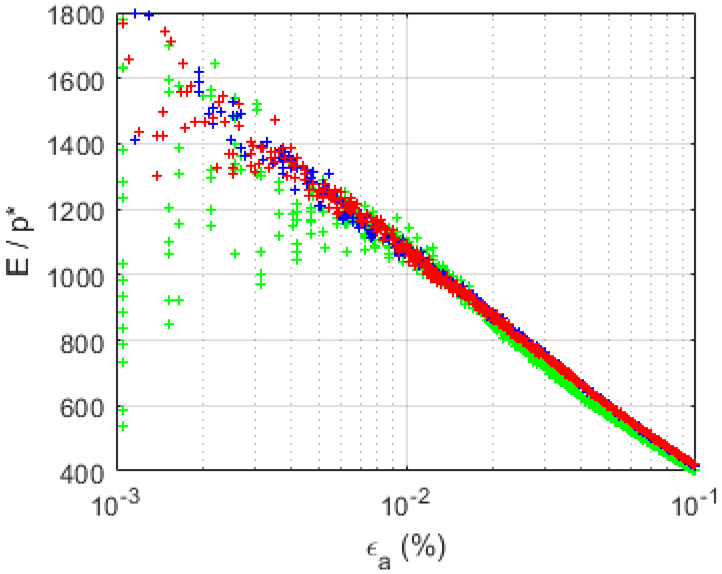

Fig. 12(b)

Fig. 12. Variation of secant modulus with axial strain for unsaturated samples at ε_a < 0.1%; (a) values normalised by ($p - u_w$); (b) values normalised by p^*.